

A Fast Computation Method for the Analysis of an Array of Metallic Nanoparticles

L. Dal Negro¹, G. Miano², G. Rubinacci², A. Tamburrino³, and S. Ventre³

¹Department of Electrical and Computer Engineering, Boston University, Boston, MA 02215 USA

²Dipartimento di Ingegneria Elettrica, Università degli Studi di Napoli Federico II, Italy

³DAEIMI, Università degli Studi di Cassino, Italy

In this paper, we present a fast computational model for the analysis of the plasmon modes in an array of metallic nanoparticles based on an efficient integral formulation of the electromagnetic problem. The full matrix describing the integral operator is sparsified by an SVD-based technique.

Index Terms—Edge elements, fast methods, integral equations, plasmon modes.

I. INTRODUCTION

SURFACE plasmon-polaritons (SPPs) are collective electron oscillations localized at the surface of metal-dielectric structures (e.g., [1] and [2]). Upon proper momentum phase-matching, propagating SPP waves can resonantly couple to electromagnetic waves at optical frequencies or can be strongly localized at the interface of metal nanostructures over deep sub-wavelength length scales.

The unique optical properties of surface plasmon polaritons enable an ample range of applications from field-enhanced optical sensing and manipulation to sub-wavelength guiding in plasmonic waveguides [3]. In particular, metallic nanoparticle arrays played an important role in the early days of plasmonics and hold tremendous promise today for the development of novel plasmonic structures [4], [5]. Therefore, accurate design methods capable to accurately describe the complex plasmon properties of large metal nanoparticle arrays are essential to the development of plasmonics technology. Computational methods, such as the discrete dipole approximation (e.g., [6]) and the finite-difference time domain (e.g., [7]), are widely used. However, in order to more accurately study the spectral properties of nanoparticle arrays frequency domain numerical methods are preferable. In particular, 3-D spectral methods enforcing the fundamental properties of the electromagnetic fields are capable to describe appropriately the plasmon resonant modes, as well as the electromagnetic field distribution near and inside arbitrarily shaped nanoparticles.

In this paper, we introduce a frequency domain numerical model based on the integral formulation of Maxwell equations for the study of plasmon modes in arbitrary arrays of metallic nanoparticles. The unknown is the induced current density distribution inside the nanoparticles. In analogy to the approach presented in [8] and [9], the current density field is split as the sum of a solenoidal and a non-solenoidal component. This kind of splitting is essential to solve the problem over a range of frequencies where the particle dimensions are much smaller than

the electromagnetic field wavelength in the hosting dielectric. The computational limits of this integral formulation are due to the necessity of assembling, storing and inverting a full matrix of large dimensions. We found very convenient to exploit its low rank property, by applying an efficient SVD based recursive scarification of the submatrices describing the interactions of well-separated blocks of unknowns.

II. NUMERICAL MODEL

The numerical method here proposed for computing the field solution of N interacting metal particles is a combination of the numerical model [9] specifically developed for treating plasmons resonances, and the recursive SVD method (see [10]–[14] and references therein), successfully applied for the fast iterative computation of the electromagnetic field from integral models. The resulting numerical method is flexible, in the sense that it allows to analyze systems made by particles having, eventually, different shapes and not embedded onto regular grids, thus making the method extremely versatile.

In this section, we briefly describe the numerical model and the SVD strategy. We assume that i) the strength of the incident field \mathbf{E}_0 is weak in order to neglect nonlinear effects, and ii) the size of the particle is much smaller than the wavelength in the host material so that the generation of bulk charge oscillations (bulk plasmons) is negligible. Under these assumptions, the metallic nanoparticles are modeled as linear isotropic dielectric objects with dielectric constant $\varepsilon(\omega)$. Thus, the solution of the electromagnetic problem is reduced to the evaluation of the of the current density field distribution

$$\mathbf{J}(\mathbf{r}) = \begin{cases} j\omega(\varepsilon - \varepsilon_0)\mathbf{E}(\mathbf{r}) & \text{in } \Omega \\ 0, & \text{otherwise} \end{cases} \quad (1)$$

where $\Omega = \bigcup_{h=1}^N \Omega_h$ and Ω_h is the region occupied by the h -th particle of the array. The field \mathbf{J} is solenoidal inside Ω and it is solution of the following integral equation [8], [9]:

$$\begin{aligned} \frac{\mathbf{J}(\mathbf{r})}{j\omega(\varepsilon - \varepsilon_0)} + j\omega\mu_0 \int_{\Omega} \mathbf{J}(\mathbf{r}')g(\mathbf{r} - \mathbf{r}')dV \\ + \frac{1}{j\omega\varepsilon_0} \nabla \left[\oint_{\partial\Omega} \mathbf{J}(\mathbf{r}') \cdot \hat{\mathbf{n}}(\mathbf{r}')g(\mathbf{r} - \mathbf{r}')dS' \right] \\ = \mathbf{E}_0(\mathbf{r})\text{in}\Omega \end{aligned} \quad (2)$$

Manuscript received October 07, 2008. Current version published February 19, 2009. Corresponding author: G. Rubinacci (e-mail: rubinacci@unina.it).

Color versions of one or more of the figures in this paper are available online at <http://ieeexplore.ieee.org>.

Digital Object Identifier 10.1109/TMAG.2009.2012758

where g is the free space Green function, $\partial\Omega = \bigcup_{h=1}^N \partial\Omega_h$, $\partial\Omega_h$ is the boundary of Ω_h , $\hat{\mathbf{n}}$ is the outward normal defined on $\partial\Omega$. As in [8] and [9] we split the unknown \mathbf{J} as the sum of two components $\mathbf{J} = \mathbf{J}_L + \mathbf{J}_S$, where \mathbf{J}_L and \mathbf{J}_S are such that $\nabla \cdot \mathbf{J}_L = \nabla \cdot \mathbf{J}_S = 0$ in Ω , $\mathbf{J}_L \cdot \hat{\mathbf{n}} = 0$ on $\partial\Omega$ and $\mathbf{J}_S \cdot \hat{\mathbf{n}} \neq 0$ on $\partial\Omega$. The term \mathbf{J}_S is responsible of the free electric charge accumulation on the surface of the metallic nanoparticles. Specifically, we represent \mathbf{J}_L and \mathbf{J}_S by means of the Whitney elements

$$\mathbf{J}_L = \sum_k I_k^L \mathbf{w}_k^L \quad (3)$$

$$\mathbf{J}_S = \sum_h I_h^S \mathbf{w}_h^S \quad (4)$$

where \mathbf{w}_k^L is the curl of the element shape function associated to an edge in the interior of Ω , whereas \mathbf{w}_h^S is the curl of an element shape function associated to an edge lying on the boundary of Ω . The selection of edge shape functions has been based on the tree-cotree decomposition of the graph made by the edges and nodes of the finite element mesh [15].

By applying the Galerkin method to (2), we obtain the following numerical model:

$$\begin{bmatrix} \tilde{\mathbf{R}}_{LL} + j\omega\tilde{\mathbf{L}}_{LL} & \tilde{\mathbf{R}}_{LS} + j\omega\tilde{\mathbf{L}}_{LS} \\ \tilde{\mathbf{R}}_{SL} + j\omega\tilde{\mathbf{L}}_{SL} & \tilde{\mathbf{D}}_{SS} + \tilde{\mathbf{R}}_{SS} + j\omega\tilde{\mathbf{L}}_{SS} \end{bmatrix} \begin{bmatrix} \mathbf{I}_L \\ \mathbf{I}_S \end{bmatrix} = \begin{bmatrix} \mathbf{V}_L \\ \mathbf{V}_S \end{bmatrix}. \quad (5)$$

where

$$\tilde{\mathbf{R}}_{\alpha,\beta} = \frac{\mathbf{R}_{\alpha,\beta}}{j\omega(\varepsilon - \varepsilon_0)}, \tilde{\mathbf{L}}_{\alpha,\beta} = \mu_0 \mathbf{L}_{\alpha,\beta}, \tilde{\mathbf{D}} = \frac{1}{\varepsilon_0} \mathbf{D} \quad (6)$$

and

$$(\mathbf{R}_{\alpha\beta})_{ij} = \int_{\Omega} \mathbf{w}_i^{\alpha}(\mathbf{r}) \cdot \mathbf{w}_j^{\beta}(\mathbf{r}) dV \quad (7)$$

$$(\mathbf{L}_{\alpha\beta})_{ij} = \int_{\Omega} \int_{\Omega} \mathbf{w}_i^{\alpha}(\mathbf{r}) \cdot \mathbf{w}_j^{\beta}(\mathbf{r}') g(\mathbf{r} - \mathbf{r}') dV' dV \quad (8)$$

$$\begin{aligned} (\mathbf{D})_{ij} &= \int_{\partial\Omega} \int_{\partial\Omega} [\mathbf{w}_i^S(\mathbf{r}) \cdot \hat{\mathbf{n}}(\mathbf{r}) \\ &\quad \times [\mathbf{w}_j^S(\mathbf{r}') \cdot \hat{\mathbf{n}}(\mathbf{r}')] g(\mathbf{r} - \mathbf{r}') dS' dS \end{aligned} \quad (9)$$

$$(\mathbf{V}_{\alpha})_i = \int_{\Omega} \mathbf{w}_i^{\alpha}(\mathbf{r}) \cdot \mathbf{E}_0(\mathbf{r}) dV. \quad (10)$$

It is worth noting that (5) is a linear system characterized by a fully populated matrix (\mathbf{L}). The solution of (5) becomes impractical by a direct method as the number of unknown grows because it requires a computational cost increasing as $O(n^3)$ and a memory occupation increasing as $O(n^2)$, n being the number of unknowns. The only manner to solve (5) is by using iterative methods such as the GMRES and, consequently, it is mandatory to reduce the computational cost for evaluating the \mathbf{L} matrix-vector product (it requires $O(n^2)$ operations by using the standard matrix-vector product formula).

Fast matrix-vector product methods such as the FMM, SVD and Pre-corrected FFT have been proved to be effective for solving large scale problems. In this work, we used the SVD based methods [10]–[14] because of its capability to efficiently

handle situations where the geometry requires a mesh with elements where one dimension is either significantly larger or smaller than the others (particles having one or two dominant dimensions). The SVD method is based on the idea that the field evaluated in a region V_E produced by a set of s sources (grouped in a different region V_S) can be described through a linear operator having a rank r decreasing as the relative separation between V_S and V_E is increased. Therefore an off-diagonal block $\underline{\mathbf{B}}$ of the matrix $\underline{\mathbf{L}}$ (a block of this type represents the interactions between sources in different regions) can be described by means of a “low” rank QR factorization. For example, if $\underline{\mathbf{B}}$ is an $m \times s$ matrix, then $\underline{\mathbf{B}} \cong \underline{\mathbf{Q}}\underline{\mathbf{R}}$ where $\underline{\mathbf{Q}}$ is $m \times r$, $\underline{\mathbf{R}}$ is $r \times s$ and r is the rank much smaller than s [12]. The computational efficiency the QR factorization can be improved by means of the modified Gram–Schmidt (MGS) procedure as proposed in [10]. In [13], a strategy adapted from the adaptive multilevel approach used to reduce the computational cost of the FMM [14], has been introduced to improve the original MGS QR-Factorization algorithm. In this strategy, a regular grid consisting of cubic cells is superimposed to the finite elements mesh. The contribution to the matrix $\underline{\mathbf{L}}$ arising from elements that belongs to non-adjacent cells is computed by means of the MGS QR-factorization method. This procedure is applied recursively by successive subdivision of each cell until the number of elements, in a given cell, is smaller than a prescribed threshold. Finally, the interactions among the elements in this cell and its adjacent cells are computed directly. At the end, by combining the MGS QR-factorization method and the multilevel procedure, we obtain a computational cost for the \mathbf{L} product that increases nearly as $O(n)$.

III. PLASMON MODES

The plasmon oscillations of the nanoparticle array are the solutions of (5) in the electric quasi-static limit $\omega \ll |(\tilde{\mathbf{R}}_{\alpha,\beta})_{i,j}|/|(\tilde{\mathbf{L}}_{\alpha,\beta})_{i,j}|$ and $g \cong g^{(0)}$, where $g^{(0)}$ is the static Green function. In this limit, (5) reduces to the system

$$\frac{1}{j\omega(\varepsilon - \varepsilon_0)} \begin{bmatrix} \mathbf{R}_{LL} & \mathbf{R}_{LS} \\ \mathbf{R}_{SL} & \frac{\varepsilon - \varepsilon_0}{\varepsilon_0} \mathbf{D} + \mathbf{R}_{SS} \end{bmatrix} \begin{bmatrix} \mathbf{I}_L \\ \mathbf{I}_S \end{bmatrix} = \begin{bmatrix} \mathbf{V}_L \\ \mathbf{V}_S \end{bmatrix} \quad (11)$$

where $\mathbf{D}^{(0)}$ is the matrix obtained by replacing g with $g^{(0)}$ in the matrix \mathbf{D} defined by (9). Since the external electric field is assumed to be almost uniform in each nanoparticle, it follows that

$$(\mathbf{V}_L)_i = \int_{\Omega} \mathbf{w}_i^L \cdot \mathbf{E}_0 dV \cong 0 \quad (12)$$

therefore

$$\mathbf{R}_{LL} \mathbf{I}_L + \mathbf{R}_{LS} \mathbf{I}_S \cong \mathbf{0}. \quad (13)$$

This implies that the electric field is conservative in a weak form. By using (6) and (13) from (11), we obtain

$$\left(\frac{\varepsilon_0}{\varepsilon - \varepsilon_0} \mathbf{A} + \mathbf{D}^{(0)} \right) \left(\frac{\mathbf{I}_S}{j\omega} \right) = \varepsilon_0 \mathbf{V}_S \quad (14)$$

where

$$\mathbf{A} = \mathbf{R}_{SS} - \mathbf{R}_{SL} (\mathbf{R}_{LL})^{-1} \mathbf{R}_{LS}. \quad (15)$$

The plasmon modes are the solutions of the homogeneous equation

$$\left(\frac{\varepsilon_0}{\varepsilon - \varepsilon_0} \underline{\underline{A}} + \underline{\underline{D}}^{(0)} \right) \underline{\underline{I}}_S = \underline{\underline{0}}. \quad (16)$$

Thus, they are the eigenvectors of the eigenvalue problem

$$\underline{\underline{D}}^{(0)} \underline{\underline{U}} = \lambda \underline{\underline{A}} \underline{\underline{U}} \quad (17)$$

and the corresponding eigenfrequencies s are the solution of the algebraic equation

$$\varepsilon(s) = \varepsilon_0 \frac{\lambda - 1}{\lambda}. \quad (18)$$

The matrices $\underline{\underline{D}}^{(0)}$ and $\underline{\underline{A}}$ are symmetric and positive definite. As consequences, the eigenvectors $\underline{\underline{U}}$ are orthonormal with respect to the scalar products $\underline{\underline{W}}^T \underline{\underline{A}} \underline{\underline{Z}}$ and $\underline{\underline{W}}^T \underline{\underline{D}}^{(0)} \underline{\underline{Z}}$, and the eigenvalues λ are positive. Furthermore, the eigenvalues verify the inequality $0 < \lambda < 1$. If the dielectric constant ε is complex (lossy metals), the eigenfrequencies s are complex, too, $s = \nu + i\mu$. Since $0 < \lambda \leq 1$ the natural modes exist only in the range of frequency where the real part of the dielectric constant is negative. For instance, for the metals described by the Drude model, we obtain

$$\nu = \omega_p \sqrt{\lambda - \frac{1}{4} \left(\frac{1}{\tau \omega_p} \right)^2}, \quad \mu = \frac{1}{2\tau} \quad (19)$$

where ω_p is the plasma frequency and τ is the relaxation time of the conduction electrons.

The solution of (14) may be represented through the eigenvectors $\underline{\underline{U}}_1, \underline{\underline{U}}_2, \dots, \underline{\underline{U}}_{N_S}$ of the generalized eigenvalue problem

$$\underline{\underline{I}}_S = \sum_h a_h \underline{\underline{U}}_h. \quad (20)$$

By substituting this expression in (14) and using (17), we obtain

$$\sum_h a_h \left(\frac{\varepsilon_0}{\varepsilon - \varepsilon_0} + \lambda_h \right) \underline{\underline{A}} \underline{\underline{U}}_h = j\omega \varepsilon_0 \underline{\underline{V}}_S. \quad (21)$$

Since the eigenvectors $\underline{\underline{U}}_1, \underline{\underline{U}}_2, \dots, \underline{\underline{U}}_{N_S}$ are orthonormal with respect to the scalar product $\underline{\underline{W}}^T \underline{\underline{A}} \underline{\underline{Z}}$ from (21), we obtain

$$a_h = j\omega \varepsilon_0 \frac{\underline{\underline{U}}_h^T \underline{\underline{V}}_S}{\frac{\varepsilon_0}{\varepsilon(\omega) - \varepsilon_0} + \lambda_h}. \quad (22)$$

The resonance frequency of the $k - th$ mode, Ω_h , is the frequency minimizing the module of the denominator in (22). For instance, for the metals described by the Drude model, we obtain

$$\Omega_h = \sqrt{\nu_h^2 - \left(\frac{1}{2\tau} \right)^2} = \omega_p \sqrt{\lambda_h - \frac{1}{2} \left(\frac{1}{\tau \omega_p} \right)^2}. \quad (23)$$

The 3-dB bandwidth of the response function is given by

$$\Delta\Omega_h = \frac{1}{\tau} \sqrt{1 + \frac{1}{4} \left(\frac{1}{\tau \Omega_m} \right)^2}. \quad (24)$$

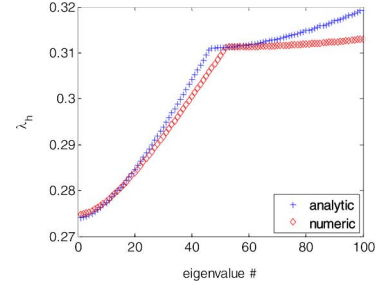


Fig. 1. Dispersion diagram: First 100 eigenvalues of a nanoparticle periodic chain with $N = 145$; + analytical and \diamond numerical evaluations.

In conclusion, once the eigenvalues and eigenvectors of the generalized eigenvalue problem (15) are known, we know all the spectral properties of the plasmon modes.

IV. NUMERICAL RESULTS AND CONCLUSIONS

As benchmark cases, we have analyzed chains of spherical nanoparticles with radius of 25 nm, aligned along the x -axis, both equally spaced (periodic array) and modulated quasi-periodically. The distance between the nanoparticle centers is 75 nm in the periodic chain. The set of distances between adjacent particles of the quasi-periodic array is composed of two values $d_A = 75$ nm and $d_B = 150$ nm. The sequence of symbols d_A and d_B are generated according to the Fibonacci inflation rule (e.g., [4]). The numerical model for 145 particles consists of 296960 elements yielding to 55535 star type unknowns [the component of the array $\underline{\underline{I}}_S$ appearing in (17)] and 566225 loop type unknown [the component of the array $\underline{\underline{I}}_L$ computed through (13)]. The leading number of eigenvalues is computed by means of the Fortran Library ARPACK for the iterative solution of large scale Eigenvalue Problems with Implicitly Restarted Arnoldi Methods (<http://www.caam.rice.edu/software/ARPACK/>) [16]. The $\underline{\underline{A}} \underline{\underline{U}}$ matrix-vector product is performed taking advantage of the sparseness of $\underline{\underline{R}}_{\alpha\beta}$ matrices and their invariance for each nanoparticle. The $\underline{\underline{D}}^{(0)} \underline{\underline{U}}$ full matrix-vector product is sparsified using the approach [12] described in the introduction, with 1.5×10^8 multiplications instead of $n^2 = 3 \times 10^9$.

The solutions evaluated by the proposed method are compared with analytical results obtained by using a simplified model based on the point dipole approximation [4], [17]. In order to compare the numerical results with those obtained analytically, the plasmon eigenmodes are characterized by the moments of the surface charges induced on the nanoparticle surfaces.

In Fig. 1, the eigenvalues obtained numerically are compared with those obtained analytically for a periodic array of 145 nanoparticles (Fig. 1). In Fig. 2, we show the distribution along the chain of the dipole moments for the array of 145 nanoparticles obtained both numerically and analytically: in Fig. 2(a), the dipole distribution corresponding to the first mode and in Fig. 2(b), the dipole distribution corresponding to the 53rd mode. The point of the dispersion curves where the slopes change abruptly separates the modes that are polarized longitudinally with respect to the chain axis, from the modes

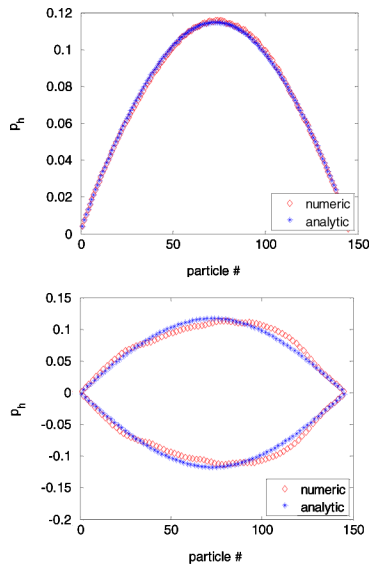


Fig. 2. (a) Dipole plasmon oscillations corresponding to the (a) first and (b) 53rd eigenvalues of a nanoparticle periodic chain with $N = 145$: +analytical and \diamond numerical evaluations.

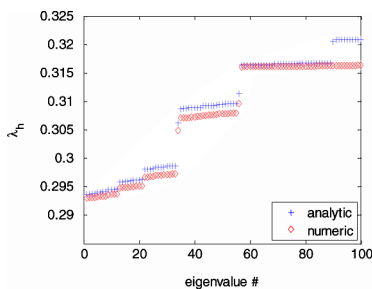


Fig. 3. Dispersion diagram of the plasmon modes in a Fibonacci chain with 145 nanoparticles: + analytical and \diamond numerical evaluations.

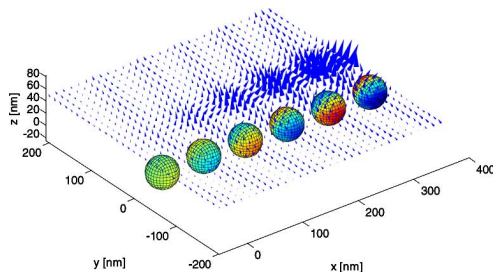


Fig. 4. Plot of the field for the first transversal mode for a regular chain of 35 nanoparticles.

that may be polarized either longitudinally or transversally. Indeed, as expected analytically, the modes corresponding to the lowest eigenvalues are polarized longitudinally with respect to the chain axis: all the modes with $h < 53$. The dipole distribution shown in Fig. 2(a) has longitudinal polarization, while the dipole distribution shown in Fig. 2(b) has transverse polarization. In Fig. 3 the first 100 eigenvalues of the Fibonacci array with 145 nanoparticles, obtained both numerically and analytically, are shown. A direct consequence of the quasi-periodicity is the appearance of gaps in the dispersion diagram,

as originally predicted in [4]. Finally, in Fig. 4, is shown the electric field for the first transversal mode (mode no. 13) for a regular chain of 35 nanoparticles.

In conclusion, we have presented a fast computational model for the 3-D analysis of the plasmon modes in array of metallic nanoparticles with arbitrary geometry, based on an efficient integral formulation of the electromagnetic problem. The full matrix describing the integral operator is sparsified by an SVD based technique. The plasmon modes excited in periodic and quasi-periodic arrays have been analyzed and the results have been compared with those obtained by the point dipole approximation [4], [17].

Further work will be addressed to the following points. First of all, by using the proposed method we shall analyze the limit of the model based on the point dipole approximation, by studying in depth the effects due to the high order dipole moments. Second, we plan to simplify the numerical model by identifying the meaningful dipole moments excited in the nanoparticles in the frequency range of interest to upgrade the point-dipole model. Finally, the effects of the dispersion and losses due to radiations on the spectral properties of the plasmon modes will be studied by generalizing the mode analysis to the full wave model.

ACKNOWLEDGMENT

This work was supported in part by the Italian MIUR.

REFERENCES

- [1] S. Lal, S. Link, and N. Halas, *Nature Photon.*, vol. 1, p. 641, 2007.
- [2] I. D. Mayergoyz, D. R. Friedkin, and Z. Zhang, *Phys. Rev. B*, vol. 72, 2005.
- [3] N.-N. Feng, M. L. Brongersma, and L. Dal Negro, *IEEE J. Quant. Electron.*, vol. 43, p. 479, 2007.
- [4] L. Dal Negro and N. Feng, *Opt. Exp.*, vol. 15, no. 22, p. 14396, 2007.
- [5] R. Dallapiccola, A. Gopinath, F. Stellacci, and L. Dal Negro, *Opt. Exp.*, vol. 16, no. 8, p. 5544, 2008.
- [6] B. T. Draine and P. J. Flatau, *J. Opt. Soc. Amer. A*, vol. 11, pp. 1491–1499, 1994.
- [7] C. Oubre and P. Nordlander, *J. Phys. Chem. B*, vol. 108, pp. 17740–17747, 2004.
- [8] G. Rubinacci and A. Tamburrino, *IEEE Trans. Antennas Propagat.*, vol. 54, pp. 2977–2989, 2006.
- [9] G. Miano, G. Rubinacci, and A. Tamburrino, *Compel*, vol. 26, pp. 586–599, 2007.
- [10] S. Kapur and D. E. Long, *IEEE Comput. Sci. Eng. Mag.*, vol. 5, pp. 60–67, 1998.
- [11] X. Sun and N. P. Pitsianis, “A matrix version of the fast multipole method,” *SIAM Rev.*, vol. 43, pp. 289–300, 2001.
- [12] R. J. Burkholder and J.-F. Lee, *IEEE Trans. Antennas Propagat.*, vol. 52, no. 7, pp. 1693–1699, Jul. 2004.
- [13] A. Maffucci, G. Rubinacci, A. Tamburrino, S. Ventre, and F. Villone, in *Proc. 23rd Annu. Rev. Progress in Applied Computational Electromagnetics*, Verona, Italy, 2007, pp. 1652–1657.
- [14] H. Cheng, L. Greengard, and V. Rokhlin, *J. Comput. Phys.*, vol. 155, pp. 468–498, 1999.
- [15] R. Albanese and G. Rubinacci, “Finite element methods for the solution of 3D eddy current problems,” in *Advances in Imaging and Electron Physics*. New York: Academic, 1998, vol. 102, pp. 1–86.
- [16] R. B. Lehoucq and A. D. C. Sorensen, *SIAM J. Matrix Anal. Appl.*, vol. 17, pp. 789–821, 1996.
- [17] C. Forestiere, G. Miano, G. Rubinacci, and L. Dal Negro, *Phys. Rev. B* 79, 085404 (2009).